Naringenin prevents cholesterol-induced systemic inflammation, metabolic dysregulation, and atherosclerosis in *Ldlr*$^{-/-}$ mice[S]

Julia M. Assini,*,† Erin E. Mulvihill,*,† Brian G. Sutherland,* Dawn E. Telford,*,§ Cynthia G. Sawyez,*,§ Sarah L. Felder,*,† Sanjiv Chhoker,*,† Jane Y. Edwards,*,§ Robert Gros,*,§, and Murray W. Huff[1],*,†,§**

Vascular Biology,* Robarts Research Institute, Department of Biochemistry,† Department of Medicine,§ and Department of Physiology and Pharmacology,** University of Western Ontario, London, Ontario, Canada

Abstract Obesity-associated chronic inflammation contributes to metabolic dysfunction and propagates atherosclerosis. Recent evidence suggests that increased dietary cholesterol exacerbates inflammation in adipose tissue and liver, contributing to the proatherogenic milieu. The ability of the citrus flavonoid naringenin to prevent these cholesterol-induced perturbations is unknown. To assess the ability of naringenin to prevent the amplified inflammatory response and atherosclerosis induced by dietary cholesterol, male *Ldlr*$^{-/-}$ mice were fed either a cholesterol-enriched high-fat or low-fat diet supplemented with 3% naringenin for 12 weeks. Naringenin, through induction of hepatic fatty acid (FA) oxidation and attenuation of FA synthesis, prevented hepatic steatosis, hepatic VLDL overproduction, and hyperlipidemia induced by both cholesterol-rich diets. Naringenin attenuated hepatic macrophage infiltration and inflammation stimulated by dietary cholesterol. Insulin resistance, adipose tissue expansion, and inflammation were alleviated by naringenin. Naringenin attenuated the cholesterol-induced formation of both foam cells and expression of inflammatory markers in peritoneal macrophages. Naringenin significantly decreased atherosclerosis and inhibited the formation of complex lesions, which was associated with normalized aortic lipids and a reversal of aortic inflammation. We demonstrate that in mice fed cholesterol-enriched diets, naringenin attenuates peripheral and systemic inflammation, leading to protection from atherosclerosis. These studies offer a therapeutically relevant alternative for the prevention of cholesterol-induced metabolic dysregulation.—Assini, J. M., E. E. Mulvihill, B. G. Sutherland, D. E. Telford, C. G. Sawyez, S. L. Felder, S. Chhoker, J. Y. Edwards, R. Gros, and M. W. Huff. **Naringenin prevents cholesterol-induced systemic inflammation, metabolic dysregulation, and atherosclerosis in *Ldlr*$^{-/-}$ mice. *J. Lipid Res.* 2013.** 54: **711–724.**

Supplementary key words cholesterol • flavonoid • lipids • obesity • hepatic steatosis • insulin resistance • metabolism

Metabolic syndrome is a collection of abnormalities, including obesity, dyslipidemia, hypertension, and insulin resistance, all of which contribute to the development of type 2 diabetes and atherosclerosis. Insulin resistance, dyslipidemia, and atherosclerosis are amplified by the development of a chronic low-grade inflammatory response (1). In insulin-resistant states, monocyte-derived macrophages infiltrate visceral adipose tissue, resulting in proinflammatory cytokine synthesis, either from adipocytes or resident macrophages, which impairs insulin sensitivity (2, 3). Administration of diets rich in saturated fats to *Ldlr*$^{-/-}$ mice represents a model with many characteristics of the metabolic syndrome (4–6). Recent studies in this

This work was supported by Heart and Stroke Foundation of Ontario (HSFO) Grants T-7707 and PG-5967 (to M.W.H.), Canadian Foundation for Innovation and Ontario Research Fund (to R.G.), a HSFO Masters Award (to J.M.A.), and a Canadian Institutes of Health Research-Canada Graduate Scholarship Doctoral Award (to E.E.M.).

Manuscript received 27 September 2012 and in revised form 14 December 2012.

Published, JLR Papers in Press, December 19, 2012
DOI 10.1194/jlr.M032631

Abbreviations: ABCG, ATP-binding cassette sub-family G; ACOX, acetyl-CoA oxidase; AP-1, activated protein 1; AUC, area under the curve; CE, cholesteryl ester; CPT-1α, carnitine palmitoyl transferase-1 alpha; CYP7A1, cholesterol 7alpha-hydroxylase; EE, energy expenditure; FC, free cholesterol; FGF21, fibroblast growth factor 21; FPLC, fast performance liquid chromatography; GTT, glucose tolerance test; HFHC, high-fat, high-cholesterol; HMGCR, 3-hydroxy-3-methyl-glutaryl-CoA reductase; IHC, immunohistochemistry; IL, interleukin; LF, low-fat; LFHC, low-fat, high-cholesterol; LXR, liver X receptor; MAPK, mitogen-activated protein kinase; MCP-1, CCL2, chemokine (C-C motif) ligand 2; CCL3, chemokine (C-C motif) ligand 3; MOMA-2, monocyte macrophage antibody 2; NF-κB, nuclear factor kappa B; PGC-1α, peroxisome proliferator-activated receptor gamma coactivator 1-alpha; RQ, respiratory quotient; SAA, serum amyloid a; SM α-actin, smooth muscle alpha actin; SREBF, sterol regulatory element-binding factor; TC, total cholesterol; TG, triglyceride; TNFα, tumor necrosis factor alpha; WAT, white adipose tissue.

[1]To whom correspondence should be addressed.
e-mail: mhuff@uwo.ca

[S] The online version of this article (available at http://www.jlr.org) contains supplementary data in the form of methods, five figures, and one table.

model have implicated elevated dietary cholesterol in the induction of macrophage infiltration and the inflammatory response in both adipose tissue and liver, leading to the exacerbation of dyslipidemia, insulin resistance, and atherosclerosis (6, 7).

Cholesterol-fed *Ldlr*$^{-/-}$ mice display increased circulating serum amyloid A (SAA), an inflammatory mediator that potentiates inflammation in the artery wall (8). In hamsters, dietary cholesterol functions synergistically with dietary fat and fructose to intensify dyslipidemia, insulin resistance, and hepatic steatosis (9). Other studies establish a link between hepatic inflammation and dyslipidemia. Tumor necrosis factor (TNF)α and interleukin (IL)-1β stimulate hepatic overproduction of apoB100-containing lipoproteins in vivo and in vitro (10, 11). Collectively, these studies indicate that a moderate increase in dietary cholesterol promotes tissue and systemic inflammation, thereby contributing to dyslipidemia, insulin resistance, and atherosclerosis. Pharmacological therapies for the treatment and prevention of the chronic low-grade inflammation associated with atherosclerosis remain elusive.

Epidemiological studies revealed an association between increased consumption of dietary flavonoids and a reduced risk of cardiovascular disease (12). Flavonoids have been shown to have anti-inflammatory properties (13). Naringenin, a citrus flavonoid, inhibits apoB100 secretion from cultured hepatocytes (14). Furthermore, in *Ldlr*$^{-/-}$ mice, addition of naringenin to a high-fat diet attenuates obesity and prevents hepatic triglyceride (TG) accumulation through increased hepatic fatty acid (FA) oxidation, leading to prevention of dyslipidemia, insulin resistance, and atherosclerosis (5, 15). These studies were performed in the context of diets low in cholesterol (0.05%). Due to the evidence that high dietary cholesterol augments the inflammatory state and potentiates atherogenesis (1), one objective of the present study was to examine the ability of naringenin to prevent these cholesterol-induced perturbations.

Diets that are low in fat but high in sucrose and contain moderate amounts of cholesterol (0.2%) induce significant atherosclerosis in *Ldlr*$^{-/-}$ mice (16). However, the effect of dietary cholesterol in low-fat diets on the local and systemic inflammatory response has not been determined. Furthermore, the ability of naringenin to prevent metabolic dysfunction and atherosclerosis in the context of a low-fat atherogenic diet remains to be elucidated. Therefore, a second objective of this study was to examine the ability of naringenin to prevent inflammation, metabolic dysregulation, and atherosclerosis in mice fed a low-fat (LF), cholesterol-containing diet.

In the current study, in *Ldlr*$^{-/-}$ mice fed either a high-fat, high-cholesterol (HFHC, 0.2%) diet or a low-fat, high-cholesterol (LFHC, 0.2%) diet, naringenin supplementation prevented dyslipidemia and hyperinsulinemia. By enhancing hepatic FA oxidation and attenuating lipogenesis, naringenin prevented hepatic steatosis. The cholesterol-induced inflammation in liver, adipose tissue, and aorta were alleviated by naringenin. Collectively, the correction of metabolic abnormalities and the inflammatory response was associated with a marked attenuation of atherosclerosis.

METHODS

Animals and diets

Male *Ldlr*$^{-/-}$ mice, 8–12 weeks of age, on a C57BL/6J background were obtained from Jackson Laboratories (Bar Harbor, ME). Mice were fed ad libitum for 12 weeks (n = 10–12/group) a standard chow diet (14% kcal fat, TD8604, Harlan Teklad, Madison, WI); a HFHC diet (42% kcal fat, 0.2% cholesterol, TD09268, Harland Teklad) ± 3% wt/wt naringenin (Sigma-Aldrich, St. Louis, MO); a LF, semisynthetic diet (12.4% kcal fat, 52% kcal sucrose, AIN-76A, Harlan Teklad); or a LFHC (12.4% kcal fat, 52% kcal sucrose, 0.2% cholesterol, TD09801, Harlan Teklad) ± 3% wt/wt naringenin. Complete dietary composition is listed in supplementary Table I. All experiments were handled in accordance with the Canadian Guide for the Care and Use of Laboratory Animals and approved by the University of Western Ontario Animal Care Committee.

Blood and tissue collection

Mice were fasted for 6 h before sacrifice. Blood and tissue collection was performed as described previously (5, 15, 17). Animals were anesthetized with Avertin, and blood was collected via cardiac puncture and stored at −20°C. Hearts were perfused with heparin-PBS, and the heart and full-length aorta were dissected together. The top half of the heart was removed, placed in optimum cutting temperature (OCT) medium and frozen on dry ice. The aorta was placed in 10% formalin. Other tissues, including liver, muscle, and adipose, were removed, weighed, snap frozen in liquid nitrogen, and stored at −80°C.

Plasma and tissue analysis

Plasma concentrations of insulin, leptin (ALPCO Diagnostics, Windham, NH), and SAA (Invitrogen, Life Technologies, Mississauga, ON) were determined by mouse-specific ELISA as per manufacturer's instructions. Plasma concentrations of TG and total cholesterol (TC) were measured enzymatically (5). The TC and TG within VLDL, LDL, and HDL particles were determined in fresh plasma by fast performance liquid chromatography (FPLC) as described previously (5). Gall bladder bile acids were measured using an enzymatic assay (18). Lipids were extracted from whole aorta and 100 mg of liver using the method of Folch et al. (19) and quantitated as described previously (20). FA and cholesterol synthesis were measured following intraperitoneal injection of [1-^{14}C]acetic acid (5). FA oxidation was determined in tissue homogenates by conversion of [^{3}H]palmitate to $^{3}H_2O$ (5).

Glucose and insulin tolerance tests

Glucose tolerance tests (GTT) were conducted in mice fasted for 6 h and injected intraperitoneally with a 15% D-glucose solution in 0.9% NaCl (1 g/kg body weight). Blood glucose was measured using a glucometer (Acenscia Elite, Bayer Healthcare, Toronto, ON) at regular intervals up to 120 min postinjection. Insulin tolerance tests (ITT) were conducted after a 5 h fast and intraperitoneal injection with 0.6 IU/kg Novolin ge Toronto (Novo Nordisk, Mississauga, ON). Blood glucose was measured as described above every 15 min for 1 h. Glucose utilization and insulin sensitivity were calculated based on the absolute area under the curve (AUC).

Triglyceride and apoB100 secretion; triglyceride and cholesterol absorption

TG and apoB100 secretion into plasma was determined following intraperitoneal injection of tyloxapol and 200 μCi of Tran [^{35}S] label (1,000 Ci/mmol, MP Biomedicals Inc., Irvine, CA) (for

apoB100 secretion only) (5). Mice were sacrificed by CO_2 inhalation, and blood was collected via cardiac puncture. A combined VLDL/IDL fraction (density < 1.019 g/ml) was isolated from 250 μl of fresh plasma by ultracentrifugation and separated on 4.5% SDS-PAGE gels (14). Intestinal cholesterol absorption was determined using a modified fecal isotope ratio method (5). Mice were gavaged with 150 μl of medium chain triglyceride oil (Novartis Medical Nutrition, Fremont, MI) containing 1 μCi of [4-^{14}C]cholesterol (Perkin Elmer, Waltham, MA) or 2.5 μCi of glycerol tri[1-^{14}C]oleate and 2.0 μCi of [5,6-^{3}H]β-sitostanol (American Radiolabeled Chemicals Inc., St. Louis, MO). Feces were collected every 24 h for three days. Fecal samples were saponified in 95% ethanol/10N KOH, neutral lipids were extracted with hexane, and the percentage of lipid absorbed was calculated as the ratio of [^{14}C] to [^{3}H] (5).

Tissue sectioning and histology

Pieces of liver were placed in OCT, frozen, and sectioned at 8 μm using a cryostat. Liver sections were stained with Oil Red O and Hoechst 33258 (2.5 μg/ml, Sigma) and visualized by fluorescence microscopy at 493 nm excitation. Immunohistochemistry (IHC) was conducted on liver sections (frozen) for the macrophage marker MAC-2 (Cedarlane, Burlington, ON). Briefly, slides were fixed in acetone, quenched with 3% H_20_2 in methanol, blocked in 10% BSA, and incubated with rat anti-mouse MAC-2 antibody (1:1000), followed by incubation with a secondary antibody (biotinylated goat anti-rat IgG antibody, 1:200, Vector, Burlington, ON). Sections were incubated in ABC reagent (Vector) followed by incubation in DAB substrate (Vector) and counterstained in hematoxylin.

White adipose tissue (WAT) was fixed in 10% formalin, embedded in paraffin, sectioned using a microtome, and stained with hematoxylin and eosin. Adipocyte diameter was calculated using Northern Eclipse 7.0 software on 20× magnification photomicrographs.

Morphometric analysis of lesions in the aortic sinus was performed as described previously (15). Frozen serial sections were stained with Oil Red O for quantitation of lesion area, and collagen was visualized by staining slides with modified Verhoff and Masson's trichrome. Macrophages were identified by IHC staining with monocyte/macrophage antibody-2 (MOMA-2, Accurate Chemical and Scientific Corporation, Westbury, NY), and smooth muscle cells were identified by staining with smooth muscle (SM) α-actin antibody (Clone 1AH, Sigma-Aldrich). The relative area of lesions positively stained for MOMA-2, collagen (trichrome), and SM α-actin was determined relative to the total area of the respective plaque. Cleaned, full-length aortas were fixed in formalin, stained with Sudan IV, prepared en face, and mounted in glycerol gelatin as described previously (15). Lesion area was calculated by dividing the stained plaque area by the total area of the aortic arch (ascending and descending aorta) and expressed as a percentage.

Gene expression analysis

Tissue mRNA levels were determined by quantitative real-time PCR as published previously (5). The expression of each gene was normalized to *Gapdh* expression, and the value of the control group (chow or LF) was set to 1.

Energy expenditure

Energy expenditure, respiratory quotient, and total activity were assessed using the Comprehensive Laboratory Animal Monitoring System (CLAMS) (Columbus Instruments, Columbus, OH). Lean body mass was calculated from whole-body composition analysis conducted by micro-CT imaging using a Locus Ultra micro-CT scanner (GE Healthcare, London, ON) (21).

Peritoneal macrophages

In a separate study, male *Ldlr*$^{-/-}$ mice 8–12 weeks of age (n = 16/group) were fed either standard chow or the HFHC diet ± 3% (wt/wt) naringenin. After 12 weeks, mice were injected intraperitoneally with 2.5 ml 4% Brewer's Thioglycollate Medium (Sigma-Aldrich); five days later, mice were sacrificed via CO_2 inhalation. Peritoneal cells were plated at a density of $2.76–3.3 \times 10^6$ per well and were allowed to adhere for 2 h (22). A subset of peritoneal cells was plated into wells containing cover slips and stained with Oil Red O. Cellular TC, cholesteryl ester (CE), and TG mass in peritoneal cells were determined enzymatically following extraction with 3:2 (vol:vol) hexane:-isopropanol (23). Cellular lipids were normalized to cell protein. Cellular mRNA levels were determined by quantitative real-time PCR (5).

Statistical analysis

Data is presented as the mean ± SEM. A one-way ANOVA and posthoc Tukey test was performed using Sigma Plot version 14.0 to determine statistical significance. Different letters indicate statistical significance ($P < 0.05$) within each separate study (chow, HFHC, and HFHC + naringenin; LF, LFHC, and LFHC + naringenin). A two-sample *t*-test was also employed to test the prespecified hypothesis that there is a significant difference ($P < 0.05$) between chow and LF groups.

RESULTS

Naringenin prevents dyslipidemia and apoB100 overproduction in cholesterol-fed mice

Hypercholesterolemia was induced in *Ldlr*$^{-/-}$ mice fed the HFHC and LFHC diets for 12 weeks, whereas naringenin supplementation reduced plasma cholesterol by more than 40% (**Table 1**). Plasma TG was significantly increased in mice fed HFHC (6-fold), LF (3-fold) and LFHC (3-fold) compared with chow. Addition of naringenin to the HFHC or LFHC diets attenuated plasma TG concentrations by ∼50% (Table 1). FPLC revealed that both cholesterol-enriched diets markedly increased VLDL- and LDL-cholesterol, and increased VLDL-TG concentrations (2- to 4-fold) (**Fig. 1A**, B). In contrast, naringenin attenuated VLDL- and LDL-cholesterol levels, and substantially reduced VLDL-TG, in the presence of either high or low dietary fat (Fig. 1A, B). Decreased plasma lipids by naringenin were independent of any effect on cholesterol or TG absorption (Table 1). The improvement in plasma lipids by naringenin was primarily due to a significant reduction in hepatic TG secretion into plasma (>55%) compared with HFHC- and LFHC-fed animals (Fig. 1C). Furthermore, HFHC- and LFHC-fed mice secreted more apoB100 (2.2- and 1.6-fold, respectively) into plasma compared with chow-fed mice. Addition of naringenin to either cholesterol-enriched diet attenuated apoB100 secretion by over 80% (Fig. 1D).

Improved liver and muscle lipid metabolism by naringenin supplementation to cholesterol-rich diets

Prominent hepatic steatosis, characterized by significantly elevated TC, CE, free cholesterol (FC), and TG

TABLE 1. Parameters in male *Ldlr*$^{-/-}$ mice after 12 weeks on diet

Metabolic Variable	Chow	HFHC	HFHC + Nar	LF	LFHC	LFHC + Nar
Final body weight (g)	28.42 ± 0.45[a]	35.51 ± 1.40[b]	27.00 ± 0.38[a]	33.32 ± 0.59[a]*	34.29 ± 0.60[a]	26.06 ± 0.56[b]
Caloric intake (kcal/day/mouse)	7.95 ± 0.67	8.70 ± 0.49	8.40 ± 0.71	11.58 ± 0.48*	11.47 ± 0.31	12.76 ± 0.38
Plasma cholesterol (mmol/l)	6.05 ± 0.22[a]	38.32 ± 3.01[b]	23.65 ± 1.95[c]	13.46 ± 0.98[a]*	46.08 ± 2.60[b]	25.64 ± 2.05[c]
Plasma TG (mmol/l)	0.66 ± 0.07[a]	3.95 ± 0.45[b]	2.17 ± 0.24[c]	1.96 ± 0.15[a]*	1.83 ± 0.18[a]	0.99 ± 0.07[b]
Plasma insulin (ng/ml)	0.20 ± 0.04[a]	0.76 ± 0.11[b]	0.23 ± 0.03[a]	0.47 ± 0.04[a]*	0.48 ± 0.11[a]	0.22 ± 0.03[b]
Blood glucose (mmol/l)	6.36 ± 0.25[a]	8.15 ± 0.33[b]	5.50 ± 0.40[a]	8.00 ± 0.45[a]*	8.39 ± 0.49[a]	5.44 ± 0.37[b]
Plasma leptin (ng/ml)	0.77 ± 0.22[a]	14.43 ± 1.69[b]	1.03 ± 0.18[a]	7.57 ± 1.19[a]*	7.55 ± 1.27[a]	0.61 ± 0.16[b]
Plasma SAA (μg/ml)	1.78 ± 0.52[a]	35.01 ± 8.76[b]	9.27 ± 3.93[a]	8.15 ± 1.72[a]*	23.04 ± 2.21[b]	5.16 ± 1.34[a]
Bile acids (gall bladder) (μmol/ml)	400 ± 60	350 ± 21	358 ± 20	382 ± 33	565 ± 48	518 ± 70
Cholesterol absorption (%)	48 ± 4.5	38 ± 2.9	42 ± 7.0	53 ± 4.3	43 ± 2.6	45 ± 3.4
Triglyceride absorption (%)	90 ± 6.2	91 ± 2.8	95 ± 1.4	93 ± 3.3	93 ± 2.0	88 ± 2.1
Activity (counts/hour)	2851 ± 193	2098 ± 117	2433 ± 194	ND	3148 ± 168	3159 ± 93
RQ	0.92 ± 0.01[a]	0.82 ± 0.01[b]	0.85 ± 0.02[b]	ND	0.96 ± 0.04	0.95 ± 0.01

Data are the mean ± SEM (n = 10–12/group). Different letters indicate statistical significance ($P < 0.05$) within either study [(Chow, HFHC, HFHC + Nar) or (LF, LFHC, LFHC + Nar)]. *$P < 0.05$ between Chow and LF. Activity; ambulatory plus stereotypic movement beam breaks over 24 h, expressed as counts per hour; Nar; naringenin; ND, not determined.

concentrations, developed in mice fed a cholesterol-rich diet compared with controls. Naringenin supplementation of the HFHC or LFHC diet decreased hepatic TC and CE (>60%) and normalized hepatic TG (**Fig. 2A**, B). Fluorescence photomicrographs of Oil Red O-stained hepatic sections revealed a substantial reduction in neutral lipid droplets in naringenin-supplemented, cholesterol-fed mice (Fig. 2C, D). Naringenin did not alter the cholesterol-induced suppression of sterol regulatory element binding protein (*Srebf) 2*, 3-hydroxy-3-methyl-glutaryl-CoA reductase (*Hmgcr*) expression (Fig. 2E, F), or hepatic cholesterol synthesis (Fig. 2G). Compared with HFHC or LFHC diets, naringenin significantly increased cholesterol 7 α-hydroxylase (*Cyp7a1*) expression (>50%) (Fig. 2E, F), suggesting increased conversion of cholesterol to bile acids. However, gall bladder bile acid content was not affected (Table 1). Naringenin did not alter hepatic expression of ATP-binding cassette subfamily G (*Abcg*) *5*, *Abcg8*, or *Abca1*, although naringenin reduced *Abcg1* mRNA compared with the HFHC or LFHC diets (supplementary Fig. I).

The HFHC and LFHC diets increased hepatic *Srebf1c* expression (4- and 1.8-fold, respectively) compared with controls, whereas naringenin significantly reduced *Srebf1c* mRNA (>30%) when added to either cholesterol-rich diet (Fig. 2E, F). De novo FA synthesis was significantly increased in cholesterol-fed animals compared with controls, whereas FA synthesis was normalized by the addition of naringenin (Fig. 2H). Compared with the HFHC or LFHC diets, naringenin increased the expression of fibroblast growth factor 21 (*Fgf21*) (3.6- and 2-fold, respectively), peroxisome proliferator-activated receptor γ coactivator 1 α (*Pgc1a*) (1.2- and 1.3-fold, respectively), and carnitine palmitoyl transferase-1 α (*Cpt1a*) (1.8- and 1.4-fold, respectively). Addition of naringenin to the LFHC diet increased acetyl-CoA oxidase 1 (*Acox1*) mRNA 2-fold, but not in mice fed HFHC plus naringenin (Fig. 2E, F). Hepatic FA oxidation was significantly increased in naringenin-supplemented mice compared with either cholesterol-enriched diet alone (Fig. 2I). In muscle, naringenin normalized the increased FA synthesis in HFHC, LF, and LFHC mice, but it did not affect muscle FA oxidation (supplementary Fig. II).

To evaluate the increased hepatic FA oxidation by the addition of naringenin to either the HFHC or LFHC diet, energy balance was assessed in an animal metabolic monitoring system. Total activity was similar among all dietary groups (Table 1). Total energy expenditure (EE) in mice fed the HFHC diet was 14% lower than that of chow-fed mice, whereas total EE was significantly increased (16%) by the addition of naringenin to the HFHC diet. Similarly, naringenin supplementation of the LFHC diet significantly increased EE (15%) compared with the LFHC diet alone (Fig. 2J and supplementary Fig. II-E). There was no significant change in caloric intake by the addition of naringenin to either the HFHC or LFHC diet (Table 1). Respiratory quotient (RQ) profiles, which reflect the relative contributions of carbohydrate and fat oxidation to total EE, were decreased in HFHC-fed mice relative to chow but were not further affected by the addition of naringenin to the HFHC. Furthermore, RQ was not changed by the addition of naringenin to the LFHC diet (Table 1). Given the significant increase in total EE in naringenin-treated mice (Fig. 2J), the lack of change of RQ profiles suggests that both fat and carbohydrate oxidation were increased in the naringenin-treated mice.

Naringenin prevents the development of cholesterol-induced hepatic inflammation

In *Ldlr*$^{-/-}$ mice, increased dietary cholesterol induces hepatic inflammation (7, 24). The HFHC diet significantly induced the expression of *Tnfa*, *Il1b*, chemokine (C-C motif) ligand 2 (*Ccl2*), chemokine (C-C motif) ligand 3 (*Ccl3*), tissue macrophage-specific marker *F4/80*, and serum amyloid a (*Saa1/2*) (**Fig. 3A**). Conversely, naringenin supplementation to the HFHC diet significantly attenuated the expression of *Tnfa*, *Il1b*, *Ccl2*, *Ccl3* (>80%) and reduced *F4/80* and *Saa1/2* mRNA (>50%) (Fig. 3A). Decreased expression of the macrophage marker F4/80 was confirmed microscopically. Enhanced hepatic macrophage accumulation (MAC-2) in HFHC-fed mice was alleviated by naringenin (Fig. 3C).

The LFHC diet also stimulated hepatic inflammatory gene expression (*Tnfa*, *Il1b*, *Ccl2*, *Ccl3*, and *Saa1/2*) and

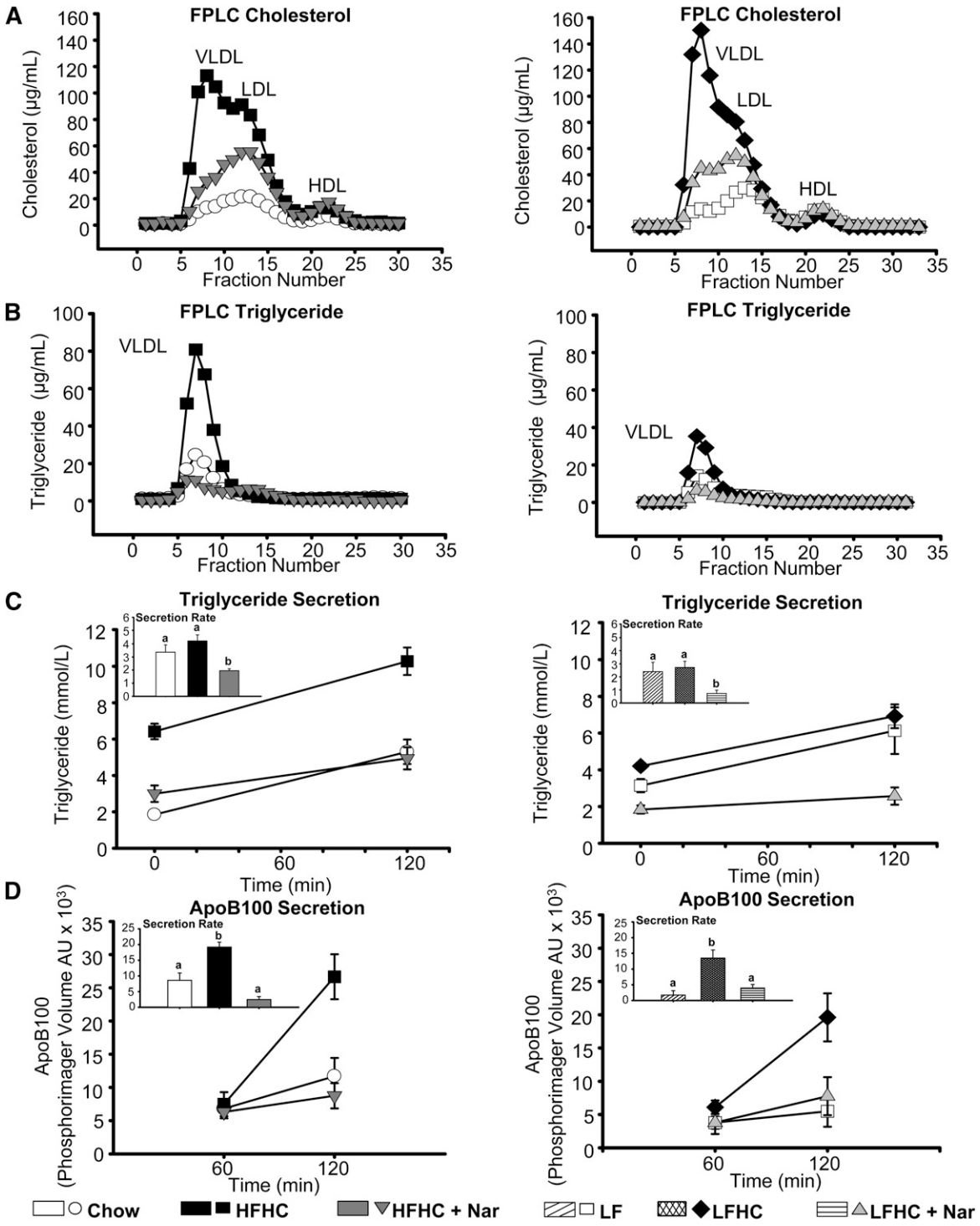

Fig. 1. Naringenin ameliorates dyslipidemia in mice fed cholesterol-rich diets. Male *Ldlr*$^{-/-}$ mice were fed chow; HFHC ± Naringenin (Nar); LF; or LFHC ± Nar for 12 weeks. (A, B) FPLC of plasma. Cholesterol and TG concentrations were measured in eluted fractions (n = 3 mice/group). (C) TG secretion at 0 and 120 min post intraperitoneal injection of tyloxapol (n = 5–6/group/time point). Inset, TG secretion rate expressed as mmol/l/h. (D) Secretion of VLDL/IDL apoB100 at 60 and 120 min post intraperitoneal injection of tyloxapol and [^{35}S]methionine (n = 5–6/group/time point). A VLDL/IDL fraction was isolated by ultracentrifugation. Inset, VLDL/IDL apoB100 secretion rate expressed as arbitrary phosphorimager volume units (AU) per hour. Values are the mean ± SEM. Different letters are statistically different ($P < 0.05$).

increased MAC-2-stained cells (Fig. 3B, D), although these increases were not as great as in HFHC mice. Naringenin treatment normalized the expression of inflammatory genes (Fig. 3B) and markedly reduced the presence of MAC-2-positive cells (Fig. 3D). Decreased hepatic *Saa1/2* expression in naringenin-treated mice was associated with a 70% reduction in plasma SAA1/2 concentrations in both dietary groups (Table 1).

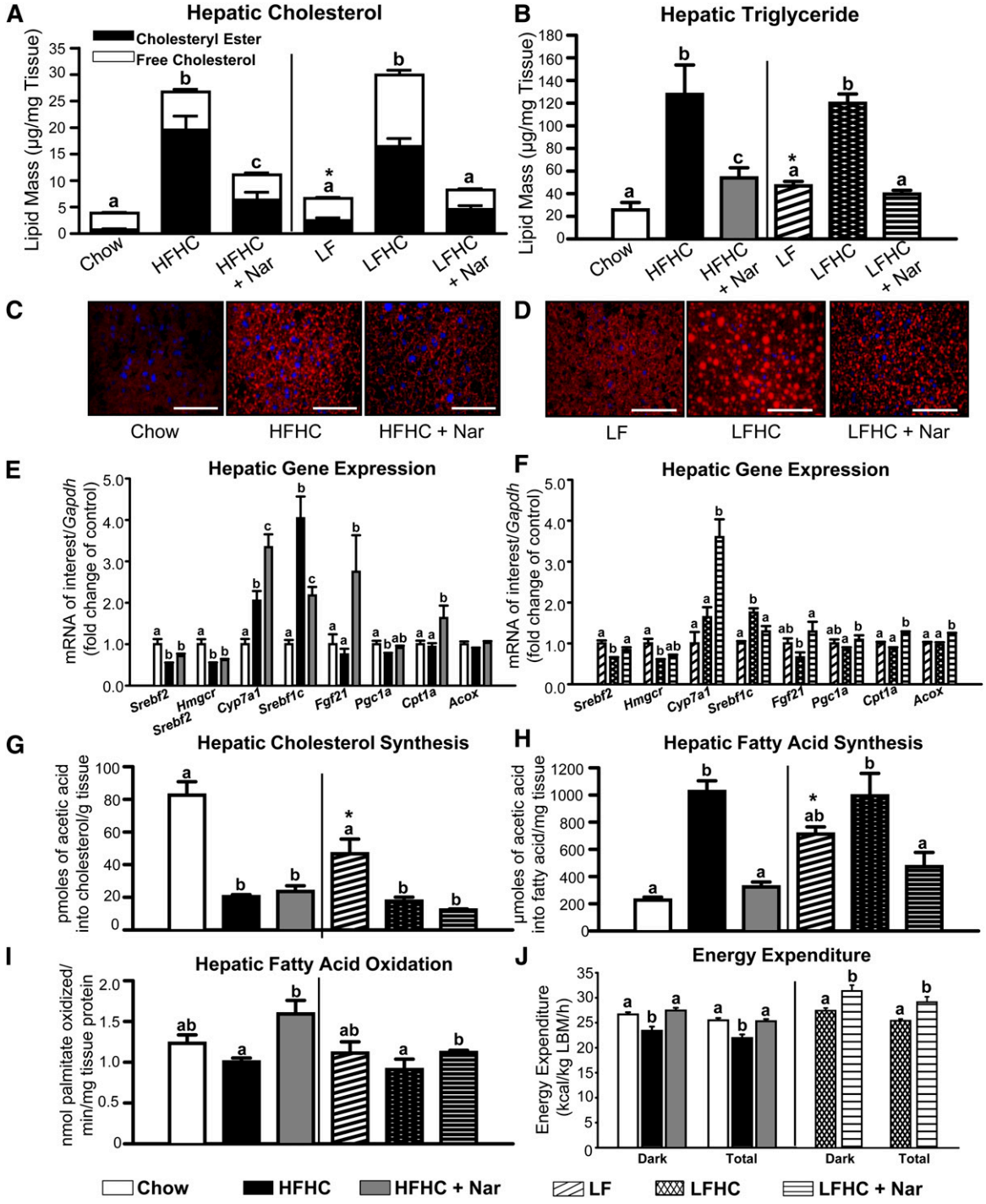

Fig. 2. Hepatic cholesterol and FA metabolism in cholesterol-fed animals with naringenin treatment. (A) Hepatic total cholesterol (whole bar), cholesteryl ester (black bar), and free cholesterol (open bar). Values are the mean ± SEM. Different letters are statistically different ($P < 0.05$) for each lipid parameter. (B) Hepatic triglyceride mass. (C, D) Representative fluorescence micrographs of liver sections stained with Oil Red O and Hoechst 33258 to visualize neutral lipid droplets (red) and nuclei (blue). Scale bar = 75 µm. (E, F) Hepatic mRNA expression (n = 10–12/group). (G) Cholesterol synthesis in the liver (n = 6–8/group) determined by incorporation of [1-^{14}C]acetic acid into cholesterol. (H) FA synthesis in the liver (n = 6–8/group) obtained 60 min post intraperitoneal injection with [1-^{14}C]acetic acid. (I) Hepatic FA oxidation (n = 6–8/group) determined by [^{3}H]palmitate conversion to H_2O. Values are the mean ± SEM. (J) Energy expenditure determined by indirect calorimetry (CLAMS system) during the light and dark cycles (7:00 PM – 7:00 AM). Measurements were collected every 10 min. Each bar represents the mean ± SEM, normalized to lean body mass (LBM) for the entire dark cycle or total 24 h period (n = 6/group). Different letters are statistically different ($P < 0.05$). * $P < 0.05$ between Chow and LF.

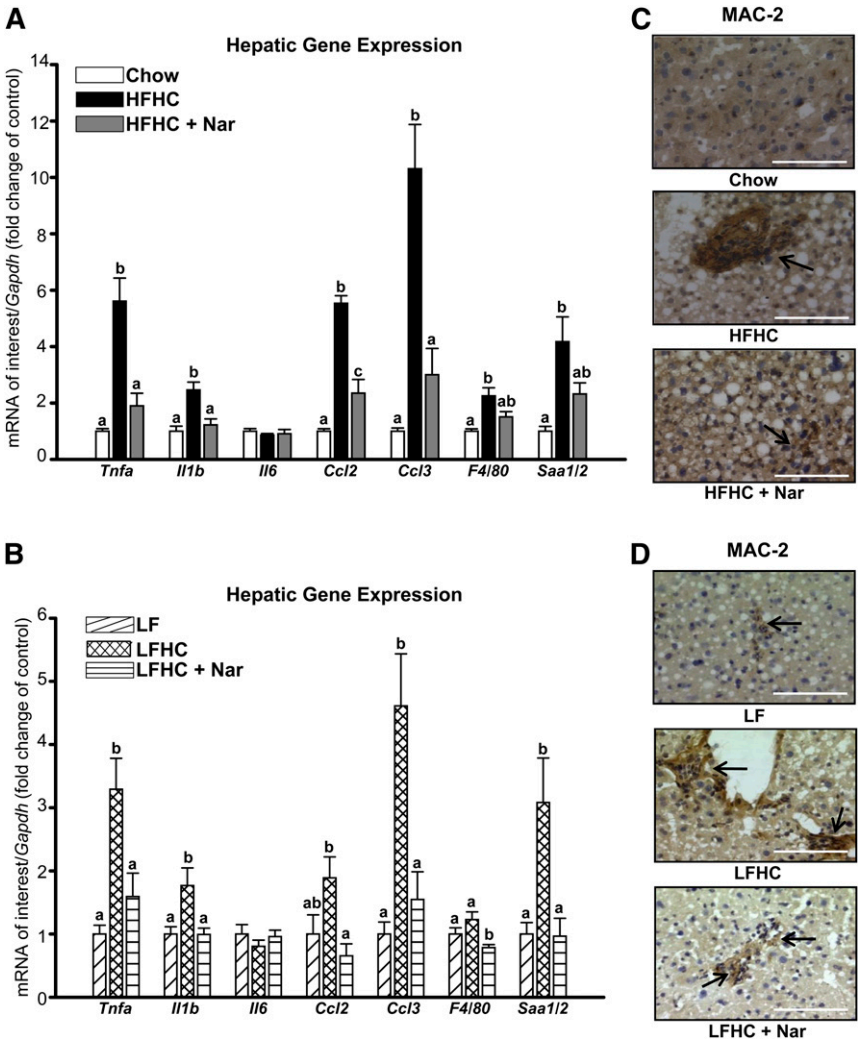

Fig. 3. Prevention of hepatic inflammation in cholesterol-fed mice supplemented with naringenin. (A, B) Hepatic mRNA expression (n = 10–12/group). (C, D) Representative photomicrographs of liver stained with MAC-2 antibody for the presence of macrophages (dark brown stain, indicated by arrows). Scale bar = 100 μm. Values are the mean ± SEM. Different letters are statistically different ($P < 0.05$).

Naringenin attenuates adipose tissue expansion and inflammation and restores glucose homeostasis in mice fed cholesterol-enriched diets

In obesity, adipocytes expand to accommodate increased TG and are associated with increased inflammation and insulin resistance (25). Dietary cholesterol may be a stimulus for both macrophage infiltration into adipose tissue and inflammatory cytokine production (6). The HFHC diet increased the adiposity index 3-fold compared with chow-fed mice (**Fig. 4A**). Both adiposity and weight gain were completely normalized by addition of naringenin to the HFHC diet (Fig. 4A and Table 1). Although the increase in adiposity index in LF-fed mice was not increased further in LFHC-fed mice, supplementation with naringenin reduced adipose tissue accumulation to the levels of chow-fed mice (Fig. 4A and Table 1). The reduction in adipose tissue by the addition of naringenin to either cholesterol-enriched diet was independent of any effect on caloric intake or TG absorption (Table 1).

The HFHC diet induced adipocyte hypertrophy (91–120 μm) compared with chow-fed mice (31–90 μm), whereas naringenin decreased adipocyte size (31–60 μm) (Fig. 4B). The LF diet increased adipocyte size (61–90 μm) compared with chow, and addition of cholesterol did not further increase adipocyte size (61–90 μm) (Fig. 4C). Naringenin treatment resulted in smaller adipocytes (31–60 μm). Concomitant with reduced adipose tissue expansion by naringenin, plasma leptin concentrations were normalized (Table 1). Expanded adipose tissue in HFHC-fed mice was associated with significantly increased expression of inflammatory genes, including *Tnfa* and *Ccl2*, and stimulated macrophage infiltration as measured by *F4/80* mRNA expression (Fig. 4D). Naringenin completely abrogated the expression of these inflammatory markers. Addition of cholesterol to the LF diet markedly induced *Tnfa*, *Il1b*, and *Ccl3* expression, demonstrating the impact of increased dietary cholesterol alone on adipose tissue inflammation (Fig. 4E). Naringenin significantly decreased *Il1b*,

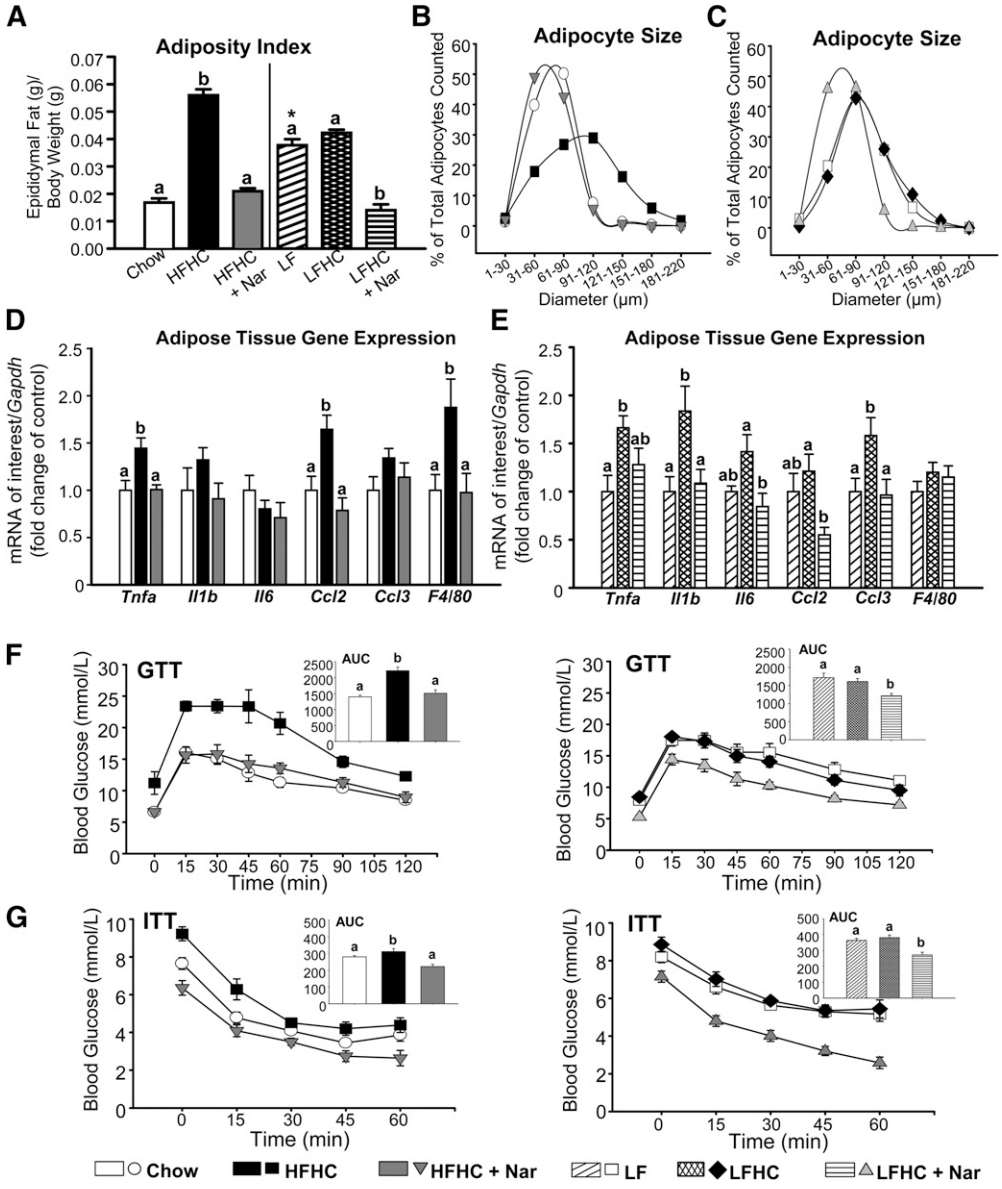

Fig. 4. Reduced adipose tissue expansion and inflammation, improved glucose homeostasis, and enhanced insulin sensitivity in naringenin-treated mice. (A) Adiposity index expressed as epididymal fat pad weight (g) normalized to body weight (g). (B, C) Adipocyte diameter distribution in epididymal fat expressed as the percentage of total adipocytes counted versus the adipocyte diameter (μm). (D, E) Adipose tissue mRNA expression (n = 8/group). (F) GTTs were performed after a 6 h fast by intraperitoneal injection of 1 g/kg glucose (n = 10–12/group). Inset: Absolute AUC, expressed as glucose (mmol/l) × 120 min. (G) ITTs were performed after a 5 h fast by intraperitoneal injection of insulin (0.6 IU/kg) (n = 10–12/group). Inset: AUC, expressed as glucose (mmol/l) × 60 min. Values are the mean ± SEM. Different letters are statistically different ($P < 0.05$). *$P < 0.05$ between Chow and LF.

Il6, *Ccl2*, and *Ccl3* mRNA compared with LFHC-fed mice. *F4/80* mRNA was unaffected, suggesting that adipose tissue macrophage infiltration in LFHC-fed mice was minimal compared with the LF diet alone (Fig. 4E).

HFHC-fed mice were modestly hyperglycemic (1.3-fold) but significantly hyperinsulinemic (3.8-fold) compared with chow-fed animals (Table 1). In contrast, naringenin completely normalized blood glucose and plasma insulin levels. The LF diet increased blood glucose (1.3-fold) and plasma insulin (2.3-fold) compared with chow. The addition of cholesterol to the LF diet did not further impact glucose or plasma insulin; however, naringenin reduced both parameters to levels observed in chow-fed mice (Table 1). Naringenin normalized both the impaired glucose tolerance and insulin sensitivity induced by the HFHC diet (Fig. 4F, G). No difference was observed in either the glucose excursion or the response to exogenous insulin between LF- and LFHC-fed mice, whereas naringenin supplementation significantly improved glucose and insulin tolerance (Fig. 4F, G).

Naringenin prevents atherosclerosis and alters plaque morphology in the aorta of cholesterol-fed mice

We next evaluated whether naringenin's ability to attenuate plasma and hepatic lipids, improve glucose and insulin homeostasis, and prevent the inflammatory response extended to protection from atherosclerosis. Compared with chow, both the HFHC and LFHC diets markedly increased Oil Red O-stained plaque area in the aortic sinus to a similar extent ($\sim$4.5 $\mu m^2 \times 10^5$) (**Fig. 5A**, B). Conversely, naringenin treatment prevented lesion development in the aortic sinus by $\sim$50% when added to either cholesterol-rich diet. Lesion area within the aortic arch was substantially increased in HFHC- and LFHC-fed mice to 14% of surface area (Fig. 5C, D). Addition of naringenin to either diet reduced plaque area by more than 40%, which is depicted in representative photographs of aortae stained with Sudan IV (supplementary Fig. III).

Analysis of lesion morphology revealed that in cholesterol-fed mice, the Oil Red O-stained lesion area was associated with MOMA-2 staining, indicating the presence of lipid-rich macrophage foam cells (supplementary Figs. IV and V). Plaques in both cholesterol-fed groups also stained positively for collagen, which corresponded to the extent of SM α-actin-stained area, suggesting that increased smooth muscle cells within lesions contributed to the secretion of collagen fibrils (supplementary Figs. IV and V). Quantitatively, the cholesterol-rich diets induced lesions in which the percentage of stained lesion area occupied by MOMA-2 was lower than controls, with a concomitant increase in the percentage area occupied by collagen and SM α-actin (Fig. 5E, F). These data suggest that cholesterol-fed mice develop complex lesions that are not only rich in lipid but also rich in collagen, representing a more fibrous phenotype. In contrast, in plaques from naringenin-fed mice, the percentage of MOMA-2-stained macrophages was elevated. These lesions contained less collagen and SM α-actin, indicative of lesions at an early stage of development (Fig. 5E, F and supplementary Figs. IV and V). Thus, in addition to reducing plaque area, naringenin attenuates the development of complex lesions.

Naringenin prevents lipid accumulation and inflammation in the aorta and in peritoneal macrophages

In aortic tissue, TC and TG mass were significantly increased in both HFHC (1.7- and 2-fold, respectively) and LFHC groups (1.5- and 2.2-fold, respectively) compared with controls (**Fig. 6A**, B). In comparison, naringenin completely prevented the cholesterol-induced deposition of aortic cholesterol and TG. The HFHC diet significantly increased expression of the inflammatory markers *Tnfa*, *Il1b*, and *Ccl2* ($\sim$2-fold) within the aortae (Fig. 6C). Conversely, naringenin supplementation of the HFHC diet normalized inflammatory cytokine expression. Aortae from the low fat-fed groups were not available for analysis of inflammatory markers.

Elicited peritoneal macrophages from $Ldlr^{-/-}$ mice fed a high-fat, 1.25% cholesterol diet have been used as an in vivo model of macrophage foam cell formation (22). We determined whether the naringenin-induced reduction in aortic lipid accumulation and inflammatory gene expression were related to a decrease in macrophage foam cell formation. Peritoneal macrophages from HFHC-fed mice accumulated significantly more CE (15-fold) and TG (4-fold) compared with macrophages from chow-fed mice (Fig. 6D). Increased lipid mass correlated with enhanced Oil Red O-stained lipid droplets (Fig. 6E). In contrast, macrophages isolated from naringenin-treated mice demonstrated a more than 50% reduction in CE and TG, correlating with a marked reduction in neutral lipid droplets. Analysis of inflammatory cytokine expression in peritoneal macrophages revealed no induction in HFHC-fed mice (Fig. 6F). Nevertheless, naringenin significantly attenuated the expression of *Tnfa*, *Ccl2*, and *Ccl3* (-30 to -50%) compared with either chow- or HFHC-fed mice (Fig. 6F). Thus, naringenin's ability to attenuate inflammation in peritoneal macrophages may, in part, be independent of its lipid-lowering properties.

DISCUSSION

Hypercholesterolemia is a significant risk factor for the development of atherosclerosis (26). In $Ldlr^{-/-}$ mice, cholesterol enrichment of high-fat diets intensifies dyslipidemia and the inflammatory response in adipose tissue and liver, which potentiates atherogenesis (1, 6, 7). Moreover, increasing the cholesterol content of low-fat, high-sucrose diets promotes hypercholesterolemia and atherosclerosis in $Ldlr^{-/-}$ mice (16). In the present study, we demonstrate that addition of naringenin to cholesterol-rich diets prevents obesity, glucose intolerance, and insulin resistance. Naringenin markedly attenuates dyslipidemia and hepatic lipid accumulation. Furthermore, naringenin alleviates the cholesterol-induced inflammatory response in liver, adipose tissue, and aorta, collectively resulting in an attenuation of atherogenesis.

Diets enriched in fat and/or cholesterol induce hepatic steatosis (7, 24), primarily a consequence of increased SREBP-1c-induced lipogenesis and reduced FA oxidation (5, 17). Furthermore, diets rich in simple carbohydrates, such as sucrose or fructose, also induce hepatic TG accumulation in rodents (9, 27). In the present study, the HFHC, LF, and LFHC diets increased hepatic FA synthesis without a compensatory increase in hepatic FA oxidation, resulting in marked hepatic steatosis compared with chow-fed mice. Addition of cholesterol to the LF diet resulted in a further increase in hepatic TG, even in the absence of excess dietary fat. Hepatic *Srebf1c* expression was also increased in LFHC-fed mice, reflecting the impact of dietary cholesterol on liver X receptor (LXR)-induced SREBP-1c-stimulated FA synthesis (28).

In contrast, naringenin reduced hepatic *Srebf1c* expression and increased *Fgf21*, *Pgc1a*, and *Cpt1a* mRNA in concert with significantly decreased hepatic FA synthesis and enhanced FA oxidation. We now demonstrate that when added to a cholesterol-enriched high-fat diet, naringenin maintains its ability to shift hepatic gene

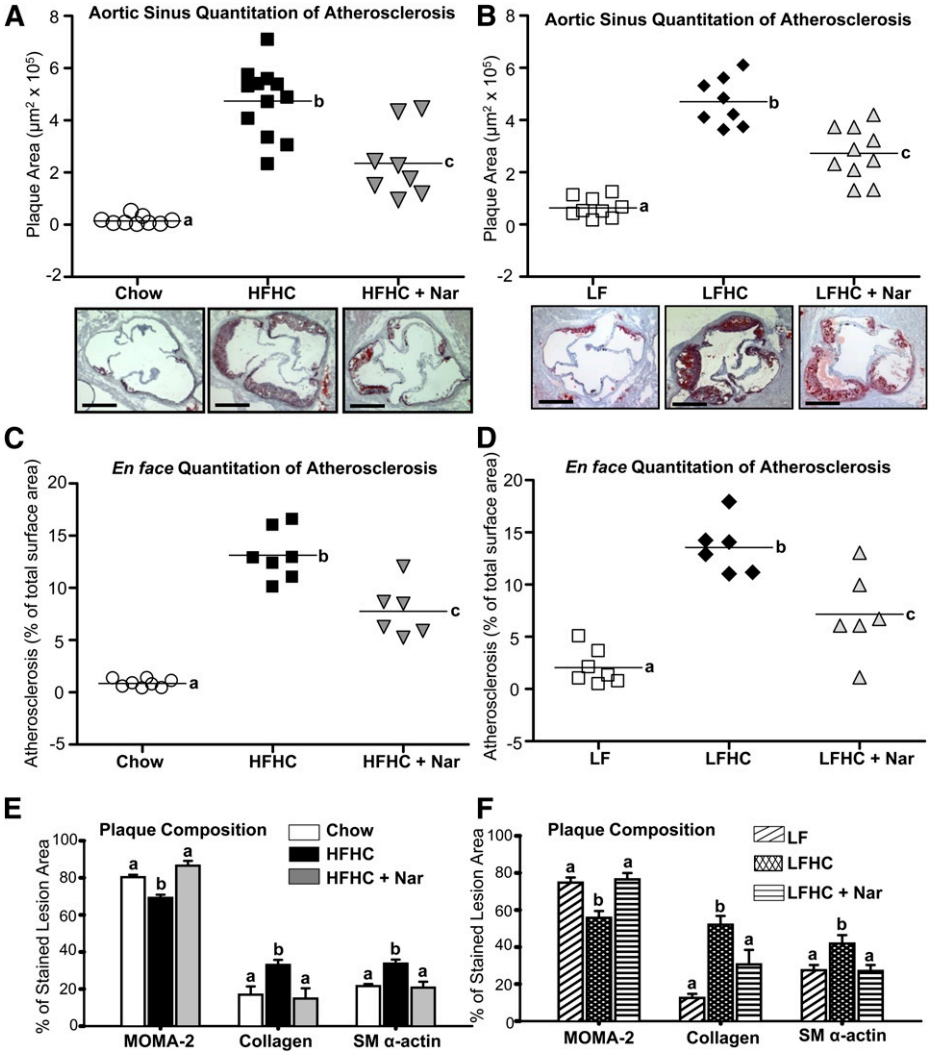

Fig. 5. Prevention of atherosclerosis in cholesterol-fed mice in the aorta by naringenin supplementation. (A, B) Plaque area ($\mu m^2 \times 10^5$) in serial sections of aortic sinus stained with Oil Red O (n = 8–10/group). Representative photomicrographs of aortic sinus stained with Oil Red O and counterstained with hematoxylin. (C, D) Atherosclerosis development in the aortic arch (percentage of Sudan IV-stained plaque area per total surface area in ascending and descending aorta; n = 6–8/group). (A–D) Values from individual mice are represented by symbols and the mean lesion area is depicted as a single horizontal line. (E, F) Graphical representation of MOMA-2 (macrophages), collagen (from trichrome), and SM α-actin-positively stained area expressed as a percentage of stained lesion area. Values are the mean ± SEM. Different letters are statistically different ($P < 0.05$).

expression to prevent hepatic TG accumulation. Furthermore, naringenin normalizes hyperinsulinemia and liver TG in mice fed a cholesterol-containing low-fat, high-sucrose diet (LFHC), primarily through diminished FA synthesis.

Hepatic apoB100 overproduction characterizes the dyslipidemia associated with insulin resistance, and increased hepatic lipid drives VLDL production (29, 30). The hepatic steatosis in HFHC- and LFHC-fed mice was associated with an overproduction of VLDL apoB100 and TG into plasma. Supplementation of either cholesterol-rich diet with naringenin abolished apoB100 oversecretion and attenuated hyperlipidemia, concomitant with the striking reduction in hepatic TG and cholesterol.

Our results are consistent with the concept that increased hepatic FA oxidation as well as decreased hyperinsulinemia-stimulated FA synthesis contributes to the naringenin-induced decrease in hepatic steatosis and VLDL overproduction, reduced adipose tissue accumulation, and normalization of muscle triglyceride levels. These observations are also consistent with studies in which genetically induced increases in hepatic FA oxidation protects mice from metabolic dysregulation. In global $Acc2^{-/-}$ mice, in which the synthesis of malonyl-CoA is blocked thus relieving the inhibition of CPT1a, hepatic FA oxidation was increased (~15%), and mice were protected from HF diet-induced hepatic steatosis, insulin resistance, and adiposity (31–34). However, this was not observed in another

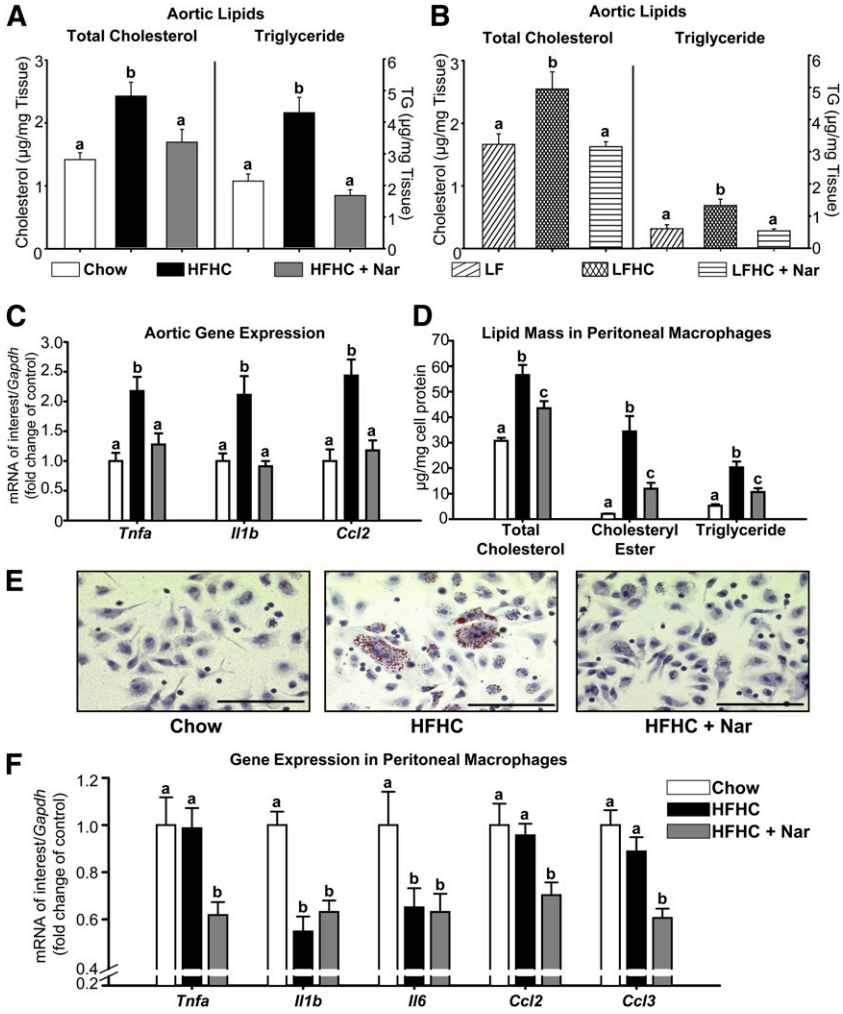

Fig. 6. Prevention of aortic lipid accumulation and inflammation in cholesterol-fed mice treated with naringenin. (A, B) Total cholesterol and triglyceride concentrations in whole aorta (n = 6–8/group). (C) mRNA expression in whole aorta (n = 6–7/group). (D) Male $Ldlr^{-/-}$ mice were fed chow or HFHC ± Nar for 12 weeks (n = 16/group), followed by intraperitoneal injection with thioglycollate. After five days, peritoneal macrophages were harvested and analyzed for cellular lipid concentrations. (E) Representative photomicrographs of peritoneal macrophages stained with Oil Red O and hematoxylin. Scale bar = 100 µm. (F) Peritoneal macrophage mRNA expression (n = 10–14/group). Values are the mean ± SEM. Different letters are statistically different ($P < 0.05$).

strain of $Acc2^{-/-}$ mice (35). Furthermore, our results are completely consistent with studies in rats (36) or mice (37) in which hepatic-specific overexpression of *Cpt1a* increased hepatic FA oxidation and protected mice from HF diet-induced hepatic steatosis and the inflammatory response as well as insulin resistance and obesity.

In this study, we assessed energy balance and found that the decrease in ectopic fat deposition in naringenin-treated mice was attributed to a ~15% increase in whole-body EE in mice fed naringenin-supplemented diets. The fact that EE was increased by naringenin while physical activity was similar in naringenin and nonnaringenin-fed mice suggests that substrate oxidation was higher with naringenin treatment. Although fat oxidation and carbohydrate oxidation are thought to be mutually inhibitory (38), similar RQ measurements were recorded for naringenin-supplemented and nonsupplemented diets, despite higher EE. This suggests that there is a simultaneous increase in both glucose and FA oxidation rather than fuel competition between fat and carbohydrate in naringenin-treated mice (34).

The cholesterol-induced inflammatory response in both liver and adipose tissue in mice fed the HFHC diet is consistent with previous reports (6, 7). The current studies demonstrate that the inflammatory response is also stimulated by addition of cholesterol to a LF diet, a model in which tissue TG accumulation is primarily derived from de novo lipogenesis. However, the magnitude of inflammatory response induced by the LFHC diet was not as great as in HFHC-fed mice, even though hepatic steatosis and adiposity were similar, suggesting that cholesterol may interact with exogenous FAs to enhance inflammation. Although both cholesterol-containing diets increased inflammatory cytokine expression, we did not distinguish which cell type (Kupffer cell, infiltrating macrophage, or adipocyte) contributed to inflammation in liver and adipose, respectively,

as each cell type can participate in the inflammatory response (25, 39).

The addition of naringenin to either the HFHC or LFHC diet substantially reduced macrophage content of liver and inflammatory cytokine expression in both liver and adipose tissue. Protection by naringenin may be through its ability to reduce cholesterol- and FA-induced lipotoxicity. Mechanisms by which dietary cholesterol might promote hepatic inflammation include increased FC, as observed in mice fed either cholesterol-containing diet. Cholesterol feeding has been shown to increase hepatic mitochondrial FC, resulting in sensitization of liver mitochondria to cytokine-mediated injury (40). Furthermore, elevated cellular FC is known to stimulate inflammatory signaling pathways in vitro, including mitogen-activated protein kinase (MAPK) and nuclear factor (NF)-κB (41). The ability of naringenin to diminish hepatic cholesterol may alleviate this inflammatory stimulus.

Incubation of adipocytes and macrophages with saturated FAs enhances inflammatory cytokine secretion, thereby linking saturated FAs to the inflammatory process (42, 43). Furthermore, diets rich in saturated fat, including the HFHC diet in the present study, induce macrophage infiltration into adipose tissue and stimulate the inflammatory response (44–46). Increased hepatic oxidation of these FAs in HF-fed mice overexpressing hepatic *Cpt1a* attenuated the expression of *Tnfa*, *Il6*, *Il1b*, and *Ccl3* in liver or adipose tissue (37). Moreover, in macrophages exposed to excess palmitate, activation of AMPK increased FA oxidation and suppressed inflammation (47). Collectively, these results suggest that naringenin's anti-inflammatory properties in adipose tissue are secondary to decreased exposure to lipoprotein-derived FAs and that naringenin's anti-inflammatory properties in liver are due to its ability to stimulate FA oxidation and/or inhibit FA synthesis. However, a direct effect of naringenin in these tissues on inflammatory signaling pathways cannot be ruled out. Naringenin has been shown to directly inhibit MAPK signaling and NF-κB activity in epithelial cells (48).

Inflammation in adipose tissue associated with obesity is thought to contribute to insulin resistance (44, 49). In *ob/ob* mice, macrophage infiltration into adipose tissue precedes the onset of hyperinsulinemia, suggesting that insulin resistance is initiated, in part, by adipose tissue inflammation (44). In vitro, TNFα inhibits insulin signaling in adipocytes, leading to reduced glucose uptake (50). In the present study, the ability of naringenin to prevent obesity and cholesterol-induced adipose tissue inflammation may contribute to the improvement in glucose homeostasis and insulin sensitivity. Two other polyphenolic molecules, resveratrol and quercetin, when incubated with human adipocytes, prevented both TNFα-mediated inflammatory cytokine secretion and inactivation of the insulin receptor (51). Further mechanistic studies are required to define any direct contribution of naringenin in adipocytes to its protection from obesity, adipose inflammation, and insulin resistance.

Obesity-associated chronic low-grade inflammation is considered a risk factor for cardiovascular disease (2, 52), and increased dietary cholesterol potentiates the inflammatory and atherogenic responses (1, 16). In HFHC- and LFHC-fed mice, increased liver and adipose tissue inflammation, combined with the development of systemic inflammation, contributed to accelerated atherogenesis compared with chow- and LF-fed mice. These mice developed lesions comprised not only of lipid-laden macrophages but also an abundance of collagen and SM α-actin, consistent with the formation of more complex lesions (53). In naringenin-treated mice, the reduced dyslipidemia, improved insulin sensitivity, and decreased hepatic, adipose, and systemic inflammation collectively contributed to a marked reduction in atherosclerosis. Lesions in naringenin-treated mice were less mature and composed mainly of macrophages, indicating that in a model in which atherogenesis is accelerated by dietary cholesterol, naringenin prevents the progression of lesions to more complex phenotypes.

Supplementation of cholesterol-rich diets with naringenin not only prevented lipid accumulation but also inflammatory cytokine expression within the aorta, demonstrating that the anti-inflammatory properties of naringenin extend to the arterial wall. Therefore, it was important to establish whether naringenin could inhibit the inflammatory response at the cellular level, specifically in macrophages, a cell that plays an integral role in mediating inflammation in lesions (54). Elicited peritoneal macrophages from HFHC-fed mice, an in vivo model of foam cell formation (22), were significantly enriched in cellular cholesterol and TG. Paradoxically, lipid accumulation was not associated with increased expression of inflammatory markers compared with chow-fed mice, indicating that macrophage lipid-loading is not necessarily linked to increased inflammation. Despite this finding, naringenin significantly attenuated peritoneal macrophage lipid content and the expression of *Tnfa*, *Ccl2*, and *Ccl3*. This implies that naringenin attenuates inflammation in macrophages not only through its ability to prevent lipid deposition but also via a direct effect on inflammatory signaling. Naringenin is known to modulate inflammation in cultured macrophages through inhibition of NF-κB and activator protein 1 (AP-1) signaling (48, 55). However, direct experimental evidence is required to elucidate the mechanisms, in addition to lipid lowering, by which naringenin prevents inflammatory signaling in macrophages, liver, and adipose tissue.

In conclusion, these studies demonstrate that naringenin prevents metabolic dysregulation induced by dietary cholesterol both in the presence and absence of dietary fat. Naringenin's potent lipid-lowering properties contribute to reduced hyperlipidemia and increased insulin sensitivity. Cholesterol-induced inflammation associated with obesity and atherosclerosis is prevented by naringenin. These studies also highlight the possibility that naringenin has a direct effect on the inflammatory processes that potentiate atherogenesis. Therefore, the beneficial effects of naringenin provide insight into possible therapeutic targets for preventing atherosclerosis associated with metabolic dysregulation.

REFERENCES

1. Subramanian, S., and A. Chait. 2009. The effect of dietary cholesterol on macrophage accumulation in adipose tissue: implications for systemic inflammation and atherosclerosis. *Curr. Opin. Lipidol.* **20:** 39–44.
2. Gustafson, B., A. Hammarstedt, C. X. Andersson, and U. Smith. 2007. Inflamed adipose tissue: a culprit underlying the metabolic syndrome and atherosclerosis. *Arterioscler. Thromb. Vasc. Biol.* **27:** 2276–2283.
3. Gutierrez, D. A., M. J. Puglisi, and A. H. Hasty. 2009. Impact of increased adipose tissue mass on inflammation, insulin resistance, and dyslipidemia. *Curr. Diab. Rep.* **9:** 26–32.
4. Merat, S., F. Casanada, M. Sutphin, W. Palinski, and P. D. Reaven. 1999. Western-type diets induce insulin resistance and hyperinsulinemia in LDL receptor-deficient mice but do not increase aortic atherosclerosis compared with normoinsulinemic mice in which similar plasma cholesterol levels are achieved by a fructose-rich diet. *Arterioscler. Thromb. Vasc. Biol.* **19:** 1223–1230.
5. Mulvihill, E. E., E. M. Allister, B. G. Sutherland, D. E. Telford, C. G. Sawyez, J. Y. Edwards, J. M. Markle, R. A. Hegele, and M. W. Huff. 2009. Naringenin prevents dyslipidemia, apolipoprotein B overproduction, and hyperinsulinemia in LDL receptor-null mice with diet-induced insulin resistance. *Diabetes.* **58:** 2198–2210.
6. Subramanian, S., C. Y. Han, T. Chiba, T. S. McMillen, S. A. Wang, A. Haw 3rd, E. A. Kirk, K. D. O'Brien, and A. Chait. 2008. Dietary cholesterol worsens adipose tissue macrophage accumulation and atherosclerosis in obese LDL receptor-deficient mice. *Arterioscler. Thromb. Vasc. Biol.* **28:** 685–691.
7. Subramanian, S., L. Goodspeed, S. A. Wang, J. Kim, L. Zeng, G. N. Ioannou, W. G. Haigh, M. M. Yeh, K. V. Kowdley, K. D. O'Brien, et al. 2011. Dietary cholesterol exacerbates hepatic steatosis and inflammation in obese LDL receptor-deficient mice. *J. Lipid Res.* **52:** 1626–1635.
8. Lewis, K. E., E. A. Kirk, T. O. McDonald, S. Wang, T. N. Wight, K. D. O'Brien, and A. Chait. 2004. Increase in serum amyloid a evoked by dietary cholesterol is associated with increased atherosclerosis in mice. *Circulation.* **110:** 540–545.
9. Basciano, H., A. E. Miller, M. Naples, C. Baker, R. Kohen, E. Xu, Q. Su, E. M. Allister, M. B. Wheeler, and K. Adeli. 2009. Metabolic effects of dietary cholesterol in an animal model of insulin resistance and hepatic steatosis. *Am. J. Physiol. Endocrinol. Metab.* **297:** E462–E473.
10. Qin, B., R. A. Anderson, and K. Adeli. 2008. Tumor necrosis factor-alpha directly stimulates the overproduction of hepatic apolipoprotein B100-containing VLDL via impairment of hepatic insulin signaling. *Am. J. Physiol. Gastrointest. Liver Physiol.* **294:** G1120–G1129.
11. Bartolomé, N., B. Arteta, M. J. Martinez, Y. Chico, and B. Ochoa. 2008. Kupffer cell products and interleukin 1beta directly promote VLDL secretion and apoB mRNA up-regulation in rodent hepatocytes. *Innate Immun.* **14:** 255–266.
12. Mulvihill, E. E., and M. W. Huff. 2010. Antiatherogenic properties of flavonoids: implications for cardiovascular health. *Can. J. Cardiol.* **26(Suppl A):** 17A–21A.
13. González, R., I. Ballester, R. Lopez-Posadas, M. D. Suarez, A. Zarzuelo, O. Martinez-Augustin, and F. Sanchez de Medina. 2011. Effects of flavonoids and other polyphenols on inflammation. *Crit. Rev. Food Sci. Nutr.* **51:** 331–362.
14. Borradaile, N. M., L. E. de Dreu, and M. W. Huff. 2003. Inhibition of net HepG2 cell apolipoprotein B secretion by the citrus flavonoid naringenin involves activation of phosphatidylinositol 3-kinase, independent of insulin receptor substrate-1 phosphorylation. *Diabetes.* **52:** 2554–2561.
15. Mulvihill, E. E., J. M. Assini, B. G. Sutherland, A. S. DiMattia, M. Khami, J. B. Koppes, C. G. Sawyez, S. C. Whitman, and M. W. Huff. 2010. Naringenin decreases progression of atherosclerosis by improving dyslipidemia in high-fat-fed low-density lipoprotein receptor-null mice. *Arterioscler. Thromb. Vasc. Biol.* **30:** 742–748.
16. Teupser, D., A. D. Persky, and J. L. Breslow. 2003. Induction of atherosclerosis by low-fat semi-synthetic diets in low density lipoprotein deficient C57BL/6J and FVB/NJ mice: comparison of lesions of the aortic root, brachiocephalic artery and whole aorta (en face measurement). *Arterioscler. Thromb. Vasc. Biol.* **23:** 1907–1913.
17. Mulvihill, E. E., J. M. Assini, J. K. Lee, E. M. Allister, B. G. Sutherland, J. B. Koppes, C. G. Sawyez, J. Y. Edwards, D. E. Telford, A. Charbonneau, et al. 2011. Nobiletin attenuates VLDL overproduction, dyslipidemia, and atherosclerosis in mice with diet-induced insulin resistance. *Diabetes.* **60:** 1446–1457.
18. Huff, M. W., D. E. Telford, J. Y. Edwards, J. R. Burnett, P. H. Barrett, S. R. Rapp, N. Napawan, and B. T. Keller. 2002. Inhibition of the apical sodium-dependent bile acid transporter reduces LDL cholesterol and apoB by enhanced plasma clearance of LDL apoB. *Arterioscler. Thromb. Vasc. Biol.* **22:** 1884–1891.
19. Folch, J., M. Lees, and G. H. Sloane Stanley. 1957. A simple method for the isolation and purification of total lipides from animal tissues. *J. Biol. Chem.* **226:** 497–509.
20. Burnett, J. R., L. J. Wilcox, D. E. Telford, S. J. Kleinstiver, P. H. Barrett, R. S. Newton, and M. W. Huff. 1997. Inhibition of HMG-CoA reductase by atorvastatin decreases both VLDL and LDL apolipoprotein B production in miniature pigs. *Arterioscler. Thromb. Vasc. Biol.* **17:** 2589–2600.
21. Granton, P. V., C. J. Norley, J. Umoh, E. A. Turley, B. C. Frier, E. G. Noble, and D. W. Holdsworth. 2010. Rapid in vivo whole body composition of rats using cone beam muCT. *J. Appl. Physiol.* **109:** 1162–1169.
22. Li, A. C., C. J. Binder, A. Gutierrez, K. K. Brown, C. R. Plotkin, J. W. Pattison, A. F. Valledor, R. A. Davis, T. M. Willson, J. L. Witztum, et al. 2004. Differential inhibition of macrophage foam-cell formation and atherosclerosis in mice by PPARalpha, beta/delta, and gamma. *J. Clin. Invest.* **114:** 1564–1576.
23. Wilcox, L. J., P. H. Barrett, R. S. Newton, and M. W. Huff. 1999. ApoB100 secretion from HepG2 cells is decreased by the ACAT inhibitor CI-1011: an effect associated with enhanced intracellular degradation of ApoB. *Arterioscler. Thromb. Vasc. Biol.* **19:** 939–949.
24. Wouters, K., P. J. van Gorp, V. Bieghs, M. J. Gijbels, H. Duimel, D. Lutjohann, A. Kerksiek, R. van Kruchten, N. Maeda, B. Staels, et al. 2008. Dietary cholesterol, rather than liver steatosis, leads to hepatic inflammation in hyperlipidemic mouse models of nonalcoholic steatohepatitis. *Hepatology.* **48:** 474–486.
25. Surmi, B. K., and A. H. Hasty. 2008. Macrophage infiltration into adipose tissue: initiation, propagation and remodeling. *Future Lipidol.* **3:** 545–556.
26. Sniderman, A. D., T. Pedersen, and J. Kjekshus. 1997. Putting low-density lipoproteins at center stage in atherogenesis. *Am. J. Cardiol.* **79:** 64–67.
27. Roncal-Jimenez, C. A., M. A. Lanaspa, C. J. Rivard, T. Nakagawa, L. G. Sanchez-Lozada, D. Jalal, A. Andres-Hernando, K. Tanabe, M. Madero, N. Li, et al. 2011. Sucrose induces fatty liver and pancreatic inflammation in male breeder rats independent of excess energy intake. *Metabolism.* **60:** 1259–1270.
28. Repa, J. J., G. Liang, J. Ou, Y. Bashmakov, J. M. Lobaccaro, I. Shimomura, B. Shan, M. S. Brown, J. L. Goldstein, and D. J. Mangelsdorf. 2000. Regulation of mouse sterol regulatory element-binding protein-1c gene (SREBP-1c) by oxysterol receptors, LXRalpha and LXRbeta. *Genes Dev.* **14:** 2819–2830.
29. Adiels, M., S. O. Olofsson, M. R. Taskinen, and J. Boren. 2008. Overproduction of very low-density lipoproteins is the hallmark of the dyslipidemia in the metabolic syndrome. *Arterioscler. Thromb. Vasc. Biol.* **28:** 1225–1236.
30. Adiels, M., M. R. Taskinen, C. Packard, M. J. Caslake, A. Soro-Paavonen, J. Westerbacka, S. Vehkavaara, A. Hakkinen, S. O. Olofsson, H. Yki-Jarvinen, et al. 2006. Overproduction of large VLDL particles is driven by increased liver fat content in man. *Diabetologia.* **49:** 755–765.
31. Abu-Elheiga, L., M. M. Matzuk, K. A. Abo-Hashema, and S. J. Wakil. 2001. Continuous fatty acid oxidation and reduced fat storage in mice lacking acetyl-CoA carboxylase 2. *Science.* **291:** 2613–2616.
32. Abu-Elheiga, L., W. Oh, P. Kordari, and S. J. Wakil. 2003. Acetyl-CoA carboxylase 2 mutant mice are protected against obesity and diabetes induced by high-fat/high-carbohydrate diets. *Proc. Natl. Acad. Sci. USA.* **100:** 10207–10212.
33. Abu-Elheiga, L., H. Wu, Z. Gu, R. Bressler, and S. J. Wakil. 2012. Acetyl-CoA carboxylase 2-/- mutant mice are protected against fatty liver under high-fat, high-carbohydrate dietary and de novo lipogenic conditions. *J. Biol. Chem.* **287:** 12578–12588.
34. Choi, C. S., D. B. Savage, L. Abu-Elheiga, Z. X. Liu, S. Kim, A. Kulkarni, A. Distefano, Y. J. Hwang, R. M. Reznick, R. Codella, et al. 2007. Continuous fat oxidation in acetyl-CoA carboxylase 2 knockout mice increases total energy expenditure, reduces fat mass, and improves insulin sensitivity. *Proc. Natl. Acad. Sci. USA.* **104:** 16480–16485.

35. Hoehn, K. L., N. Turner, M. M. Swarbrick, D. Wilks, E. Preston, Y. Phua, H. Joshi, S. M. Furler, M. Larance, B. D. Hegarty, et al. 2010. Acute or chronic upregulation of mitochondrial fatty acid oxidation has no net effect on whole-body energy expenditure or adiposity. *Cell Metab.* **11:** 70–76.
36. Stefanovic-Racic, M., G. Perdomo, B. S. Mantell, I. J. Sipula, N. F. Brown, and R. M. O'Doherty. 2008. A moderate increase in carnitine palmitoyltransferase 1a activity is sufficient to substantially reduce hepatic triglyceride levels. *Am. J. Physiol. Endocrinol. Metab.* **294:** E969–E977.
37. Orellana-Gavaldà, J. M., L. Herrero, M. I. Malandrino, A. Paneda, M. Sol Rodriguez-Pena, H. Petry, G. Asins, S. Van Deventer, F. G. Hegardt, and D. Serra. 2011. Molecular therapy for obesity and diabetes based on a long-term increase in hepatic fatty-acid oxidation. *Hepatology.* **53:** 821–832.
38. Randle, P. J., P. B. Garland, E. A. Newsholme, and C. N. Hales. 1965. The glucose fatty acid cycle in obesity and maturity onset diabetes mellitus. *Ann. N. Y. Acad. Sci.* **131:** 324–333.
39. Huang, W., A. Metlakunta, N. Dedousis, P. Zhang, I. Sipula, J. J. Dube, D. K. Scott, and R. M. O'Doherty. 2010. Depletion of liver Kupffer cells prevents the development of diet-induced hepatic steatosis and insulin resistance. *Diabetes.* **59:** 347–357.
40. Marí, M., F. Caballero, A. Colell, A. Morales, J. Caballeria, A. Fernandez, C. Enrich, J. C. Fernandez-Checa, and C. Garcia-Ruiz. 2006. Mitochondrial free cholesterol loading sensitizes to TNF- and Fas-mediated steatohepatitis. *Cell Metab.* **4:** 185–198.
41. Li, Y., R. F. Schwabe, T. DeVries-Seimon, P. M. Yao, M. C. Gerbod-Giannone, A. R. Tall, R. J. Davis, R. Flavell, D. A. Brenner, and I. Tabas. 2005. Free cholesterol-loaded macrophages are an abundant source of tumor necrosis factor-alpha and interleukin-6: model of NF-kappaB- and map kinase-dependent inflammation in advanced atherosclerosis. *J. Biol. Chem.* **280:** 21763–21772.
42. Suganami, T., K. Tanimoto-Koyama, J. Nishida, M. Itoh, X. Yuan, S. Mizuarai, H. Kotani, S. Yamaoka, K. Miyake, S. Aoe, et al. 2007. Role of the Toll-like receptor 4/NF-kappaB pathway in saturated fatty acid-induced inflammatory changes in the interaction between adipocytes and macrophages. *Arterioscler. Thromb. Vasc. Biol.* **27:** 84–91.
43. Anderson, E. K., A. A. Hill, and A. H. Hasty. 2012. Stearic acid accumulation in macrophages induces toll-like receptor 4/2-independent inflammation leading to endoplasmic reticulum stress-mediated apoptosis. *Arterioscler. Thromb. Vasc. Biol.* **32:** 1687–1695.
44. Xu, H., G. T. Barnes, Q. Yang, G. Tan, D. Yang, C. J. Chou, J. Sole, A. Nichols, J. S. Ross, L. A. Tartaglia, et al. 2003. Chronic inflammation in fat plays a crucial role in the development of obesity-related insulin resistance. *J. Clin. Invest.* **112:** 1821–1830.
45. Weisberg, S. P., D. McCann, M. Desai, M. Rosenbaum, R. L. Leibel, and A. W. Ferrante, Jr. 2003. Obesity is associated with macrophage accumulation in adipose tissue. *J. Clin. Invest.* **112:** 1796–1808.
46. Coenen, K. R., M. L. Gruen, A. Chait, and A. H. Hasty. 2007. Diet-induced increases in adiposity, but not plasma lipids, promote macrophage infiltration into white adipose tissue. *Diabetes.* **56:** 564–573.
47. Galic, S., M. D. Fullerton, J. D. Schertzer, S. Sikkema, K. Marcinko, C. R. Walkley, D. Izon, J. Honeyman, Z. P. Chen, B. J. van Denderen, et al. 2011. Hematopoietic AMPK beta1 reduces mouse adipose tissue macrophage inflammation and insulin resistance in obesity. *J. Clin. Invest.* **121:** 4903–4915.
48. Yang, J., Q. Li, X. D. Zhou, V. P. Kolosov, and J. M. Perelman. 2011. Naringenin attenuates mucous hypersecretion by modulating reactive oxygen species production and inhibiting NF-kappaB activity via EGFR-PI3K-Akt/ERK MAPKinase signaling in human airway epithelial cells. *Mol. Cell. Biochem.* **351:** 29–40.
49. Hotamisligil, G. S., P. Peraldi, A. Budavari, R. Ellis, M. F. White, and B. M. Spiegelman. 1996. IRS-1-mediated inhibition of insulin receptor tyrosine kinase activity in TNF-alpha- and obesity-induced insulin resistance. *Science.* **271:** 665–668.
50. Hotamisligil, G. S., D. L. Murray, L. N. Choy, and B. M. Spiegelman. 1994. Tumor necrosis factor alpha inhibits signaling from the insulin receptor. *Proc. Natl. Acad. Sci. USA.* **91:** 4854–4858.
51. Chuang, C. C., K. Martinez, G. Xie, A. Kennedy, A. Bumrungpert, A. Overman, W. Jia, and M. K. McIntosh. 2010. Quercetin is equally or more effective than resveratrol in attenuating tumor necrosis factor-{alpha}-mediated inflammation and insulin resistance in primary human adipocytes. *Am. J. Clin. Nutr.* **92:** 1511–1521.
52. Berg, A. H., and P. E. Scherer. 2005. Adipose tissue, inflammation, and cardiovascular disease. *Circ. Res.* **96:** 939–949.
53. Whitman, S. C. 2004. A practical approach to using mice in atherosclerosis research. *Clin. Biochem. Rev.* **25:** 81–93.
54. Tabas, I. 2010. Macrophage death and defective inflammation resolution in atherosclerosis. *Nat. Rev. Immunol.* **10:** 36–46.
55. Bodet, C., V. D. La, F. Epifano, and D. Grenier. 2008. Naringenin has anti-inflammatory properties in macrophage and ex vivo human whole-blood models. *J. Periodontal Res.* **43:** 400–407.